Hierarchical structural gradients in injection moulded poly(ethylene naphthalene-2,6-dicarboxylate) parts

Yakup Ülçer and Mükerrem Çakmak*
Polymer Engineering Institute, College of Polymer Science and Polymer Engineering, The University of Akron, Akron, OH 44325-0301, USA
(Received 26 April 1994; revised 8 June 1994)

Structural development in injection moulded poly(ethylene naphthalene-2,6-dicarboxylate) (PEN) was studied as a function of processing parameters including mould temperature, injection speed and holding time. This polymer exhibits a relatively low thermal crystallization rate and as a result quenches into wholly amorphous form when moulded into thick cavities at low mould temperatures. It, however, exhibits a three-layer structural gradient (an amorphous skin, a shear crystallized intermediate layer and an amorphous core) when moulded into thin cavities at mould temperatures up to about its cold crystallization temperature. Above this temperature, thermally activated crystallization starts playing a role particularly in the structural formation at the interior of the samples. At these temperatures the holding time in the mould becomes an important factor and as it gets longer the overall crystallinity in the sample increases. Thermal analysis results suggested that at mould temperatures up to its glass transition temperature the crystal structure of PEN consists of a mixture of ordinary α form and β form that exhibits high melting temperature. Mechanical properties of injection moulded PEN were found to mostly depend on mould temperature and at high moulding temperatures on holding time.

(Keywords: PEN; injection moulding; morphology)

INTRODUCTION

Poly(ethylene naphthalene-2,6-dicarboxylate) (PEN) is a slowly crystallizing semicrystalline aromatic polycondensate having the repeat unit:

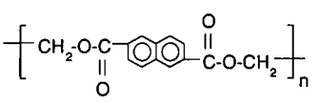

This polymer was first synthesized by ICI in 1948[1] and since then has been studied by various groups[2-9]. Inclusion of the naphthalene group in the chain provides rigidity and thus results in a high glass transition temperature ($T_g = 118°C$), melting temperature ($T_m = 270°C$) as well as related mechanical properties including tensile modulus, strength and creep resistance.

PEN can be formed into amorphous form by rapid quenching from the melt, and it can be crystallized by stress or thermal effects, or by a combination of both. The usually observed crystallinity is ~45%. Engineering properties of PEN were described by Ouchi *et al.*[2]. Unlike poly(ethylene terephthalate) (PET), PEN exhibits relatively high melt viscosity which lends itself to be used in processing operations requiring high melt strength such as fibre spinning, extrusion blow moulding and tubular film blowing.

PEN is known to have two different triclinic crystal forms[3]. The most common and well studied α form has the following unit cell[4]: $a = 0.651$ nm, $b = 0.575$ nm, $c = 1.32$ nm, $\alpha = 81.33°$, $\beta = 144°$ and $\gamma = 100°$. The formation of the β form was first reported by Zachmann *et al.*[5], and it occurs during crystallization at temperatures above 245°C. The unit cell parameters of the β form were reported by Buchner *et al.*[3] to be: $a = 0.926$ nm, $b = 1.559$ nm, $c = 1.273$ nm, $\alpha = 121.6°$, $\beta = 95.57°$ and $\gamma = 122.52°$. However, a detailed crystal structure of the β form is yet to be published.

Thermal analysis of PEN samples having different crystallinity and thermal history was carried out by Cheng and Wunderlich[6]. The melting behaviour of PEN was found to depend strongly on the crystallization history. The estimated equilibrium thermal parameters of PEN are: heat of fusion, $\Delta H° = 25 \pm 2$ kJ mol^{-1}, entropy of fusion of 100% crystalline PEN, $\Delta S^0 = 41 \pm 3.3$ J kmol^{-1} and equilibrium melting temperature, $T_m^0 = 337°C$.

The crystallization and melting behaviour of PEN was investigated by Zachmann *et al.*[5] and Buchner *et al.*[3] using d.s.c. and synchrotron radiation. They found that at crystallization temperatures up to 200°C only the α crystal modification is formed. Above this temperature the β crystal modification was obtained if the material had been molten at 280°C while the α modification was formed if the temperature of the melt was raised to 320°C. The half times of crystallization as a function of temperature showed a broad minimum ranging from 180

* To whom correspondence should be addressed

0032-3861/94/26/5651-21

to 240°C. They observed that applying a special annealing procedure raises the melting points of both crystal modifications from 272 to 290°C.

Cheng *et al.* studied the stress induced crystallization in uniaxially drawn PEN films[7]. They found that the crystallization temperature peak, heat of crystallization and heat of fusion were strongly dependent on drawing conditions. Ghanem and Porter[8] conducted isothermal solid state coextrusion above and below the T_g using the split-billet method. They found that the onset of cold crystallization of drawn PEN depends on the extent of orientation and prior crystallinity. The exothermic cold crystallization peak and T_g were affected by the extrusion conditions.

Çakmak and co-workers[9] studied uni- and biaxially stretched PEN films. They observed an unusual necking behaviour at temperatures as high as 30°C above the T_g. This caused large thickness non-uniformities in the films stretched to intermediate stretch ratios. When they were stretched past the strain hardening point the 'self levelling effect' due to strain hardening allowed uniform high quality films to be obtained. Stretching at higher temperatures resulted in the elimination of both necking and stress hardening unless high draw rates were used. This behaviour resulted in a narrowing of the processing window in which films of uniform quality occur. In this class of slowly crystallizing polymers this optimum processing window spans the temperatures between T_g and the cold crystallization temperature (T_{cc}) as in the case of PET[10], poly(*p*-phenylene sulfide)[11] (PPS), poly(ether ether ketone)[12] (PEEK) and poly(aryl ether ketone)[13] (PAEK). The uniformity of the films was found to depend on stretch ratio(s), mode, rates and temperature. Wide-angle X-ray scattering (WAXS) studies on PEN showed that the chains are packed in the α crystal modification in all stretched and annealed films. WAXS pole figure analysis also indicated that the flat faces of the naphthalene groups are aligned parallel to the film surface. Finally, Çakmak *et al.* reported that the mechanical properties of PEN were enhanced by high biaxial draw ratios followed by annealing.

Injection moulding is one of the most important processing operations in the rapid manufacturing of identical polymeric materials. It involves non-isothermal transient flow of non-Newtonian fluids in complex geometries with simultaneous structuring and solidification which usually accompanies severe thermal and deformation gradients. The process characteristics[14] and structure property relationships were studied in detail in the case of rapidly crystallizing polymers[15] such as polyethylene (PE), poly(ethylene oxide) (PEO) and polypropylene (PP). Recently the structures developed during injection moulding of slowly crystallizing polymers consisting of aromatic polycondensates such as PPS[11], PEEK[12] and PAEK[13] and their simulation[16] have been studied. In this paper our results on the processing, structure and property relationships in injection moulding of PEN will be presented.

EXPERIMENTAL

Material

The PEN used in this study was provided by Goodyear Co. under the trade name Traytuf HP, VFR40008X. It is an injection moulding grade PEN having an intrinsic viscosity of 0.824 dl g^{-1}. The PEN pellets were dried in a vacuum oven at 145°C for at least 24 h and processed immediately after drying.

The shear viscosity of PEN was determined at 290, 300 and 310°C using an Instron capillary rheometer. To prevent degradation during rheometric measurements, the barrel of the rheometer was blanketed with argon gas. A die having a diameter of 0.762 mm and a length to diameter ratio of 27.95 was used for the measurements. The data were corrected for frictional losses but the end effects were neglected.

Injection moulding

End-gated ASTM small dumb-bells were injection moulded at four different mould temperatures (20, 90, 120 and 180°C) using a Boy 15S injection moulding machine. The feeding section of the machine was purged with nitrogen gas to prevent degradation. At each mould temperature three different injection speeds (2.10, 3.45 and 5.00 cm s^{-1}) were used. The material was moulded with a packing time of 5 s and a holding time of 30 s. However, at the mould temperature of 180°C where the effect of thermal crystallization was studied the holding times were 5, 10, 20 and 30 min. A 30-s holding time could not be used at this temperature, since it was impossible to eject the material without crystallizing it. All processing variables are summarized in *Table 1*.

Cutting procedures

To characterize the structure of the injection moulded test bars three sectioning procedures were used. *Figure 1* shows the dimensions of the small dumb-bell together with schematic diagrams of the cutting procedures. Procedure A1 involved cutting sections of 0.2–0.6 mm thickness perpendicular to the flow direction for optical and d.s.c. studies. Procedure A2, which is a variation of Procedure A1, consisted of cutting slices along the width direction and microtoming layers form these cuts along the thickness direction. Finally, Procedure B consisted of cutting slices form the centre of the specimen along the flow direction. The samples were cut using a Leco VC-50 diamond saw and microtomed using a Reichert-Jung 2050 motorized microtome.

Optical microscopy

Optical photomicrographs of the samples cut using Procedures A1 and B were taken in transmission mode using a Nikon FM camera equipped with a close-up lens.

Table 1 Injection moulding conditions

Barrel temperature (°C)	
Zone I	285
Zone II	290
Nozzle temperature (°C)	90% of the barrel temperature
Mould temperature (°C)	20, 90, 120, 180
Injection pressure (MPa)	13.79
Back pressure (MPa)	0
Injection speed (cm s^{-1})	
High	5.00
Medium	3.45
Low	2.10
Packing time (s)	5
Holding time (s)	30, 300, 600, 1200, 2400
Screw rotation speed (rev min^{-1})	230
Clamping force (t)	15

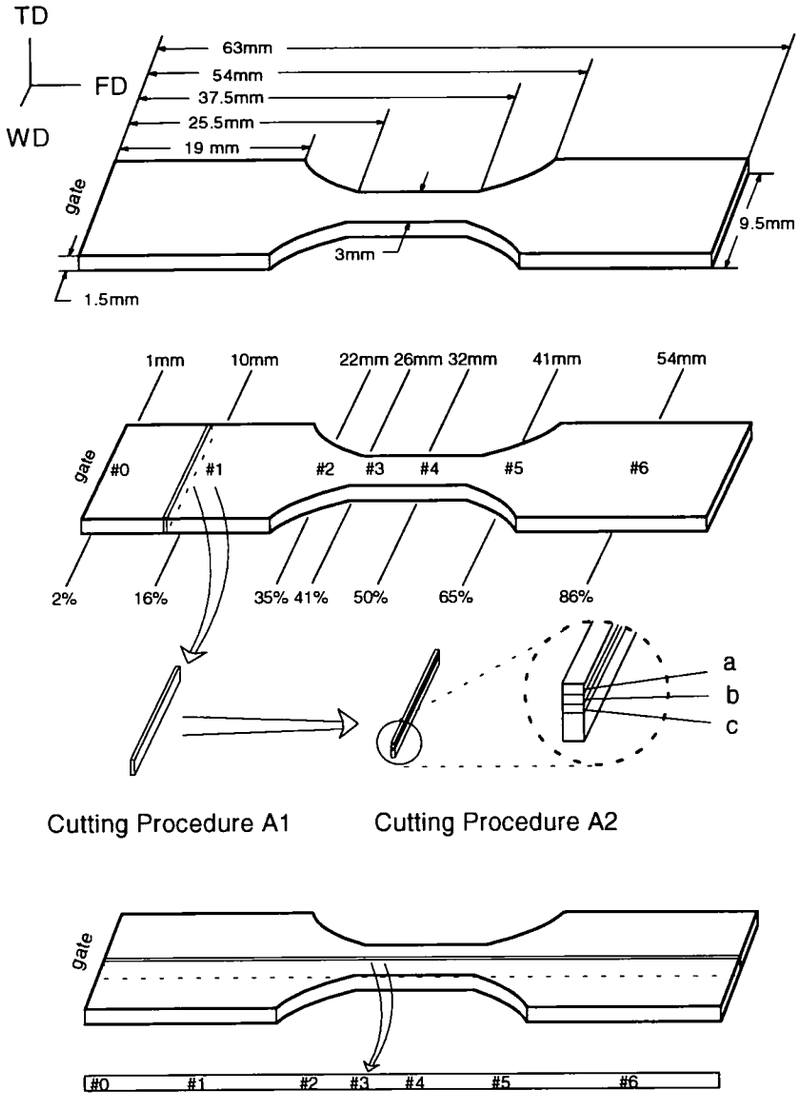

Figure 1 Dimensions of the cavity and schematic diagrams of Procedures A and B

The thickness of the observed layers were measured using a Leitz Laborlux 12 POL S polarizing microscope fitted with a measuring eyepiece.

Thermal characterization

The endothermic crystallization peak of PEN is known to be strongly influenced by heating rate[5,6]. In order to determine the heating rate which will allow an accurate determination of the degree of crystallinity, we scanned crystalline and quenched PEN samples at heating rates of 5, 10 and 20°C min^{-1}. A heating rate of 10°C min^{-1} was found to be most effective in determining the areas of the endothermic melting peak and exothermic crystallization peak. Thermal analysis of the samples cut using Procedures A1 and A2 was performed on a Perkin–Elmer DSC model 7. The edges of the sampls were cut to eliminate the end effects. The percentage crystallinity X of the samples was determined from:

$$X = \frac{\Delta H_{exp}}{\Delta H^0} \quad (1)$$

where $\Delta H_{exp} = \Delta H_m - \Delta H_c$ and ΔH^0 is the heat of fusion of 100% crystalline PEN ($\Delta H^0 = 103.4 \pm 8.29$ J g^{-1})[6].

A Mettler FT-84 hot stage was used to study the melting behaviour of the injection moulded samples. Again a heating rate of 10°C min^{-1} was used. Samples having a thickness of 20 μm were microtomed from location no. 3 using A1 and B cuts and placed in the hot stage. The hot stage was placed at 45° to the cross polars of the Leitz polarized microscope. The melting sequence was recorded using a Sony 3-chip charge-coupled detector camera connected to a video recorder.

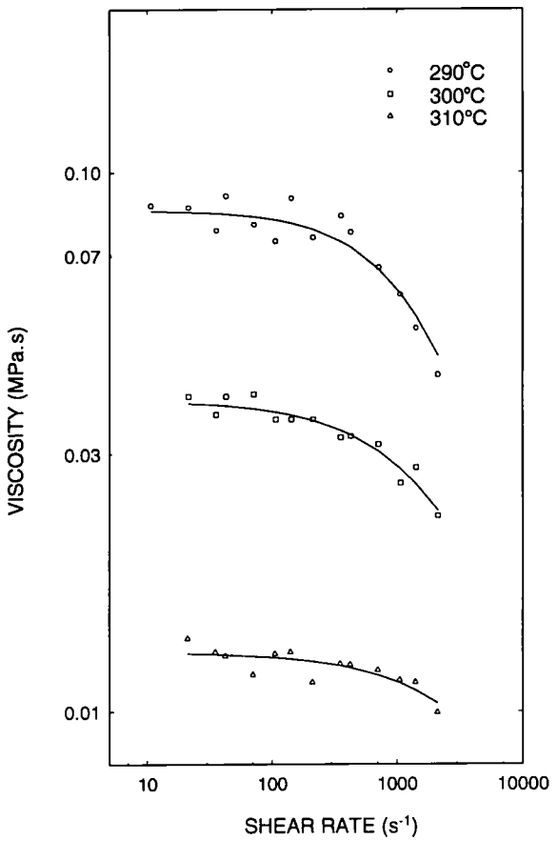

Figure 2 Apparent viscosity of PEN as a function of shear rate at different temperatures

Tensile testing

The tensile testing of the samples moulded at various processing conditions was performed using an Instron 4204 series IX automated tensile tester. The 26 mm gauge samples were tested with a testing rate of 10% min^{-1} and a testing temperature of 22°C (room temperature).

Scanning electron microscopy

The fracture surfaces of tensile tested samples were studied using an ISI model SX-40 scanning electron microscope. The samples were sputter-coated with a gold palladium alloy before viewing under the microscope.

RESULTS AND DISCUSSION

Rheological behaviour

The shear viscosity of PEN as a function of shear rate at three different temperatures is shown in *Figure 2*. We can observe a Newtonian plateau at low shear rates. At high shear rates the viscosity decreases as expected and material shows non-Newtonian behaviour. Temperature has a significant effect on the width of the Newtonian plateau and on the magnitude of viscosity. As expected, viscosity decreases with increasing temperature. Also the material becomes more Newtonian as the temperature increases as indicated by the widening of the Newtonian plateau region at low shear rate regions.

The study of the temperature dependence of the viscosity of the polymer is most important to the understanding of the mechanism of their flow process, especially in non-isothermal processes such as melt spinning and injection moulding. The temperature dependence of viscosity may be represented by the Arrhenius-Frenkel-Eyring (AFE) formula[17]:

$$\eta_{(\text{shear-stress})} = A \exp\left(\frac{\Delta E}{RT}\right) \quad (2)$$

where ΔE is the activation energy of the flow process, A is a constant, R is the gas constant, T is the temperature and η is the apparent viscosity at constant shear stress. The activation energy of PEN as a function of shear stress is shown in *Table 2*. The activation energy of flow is related to the flexibility of the chain and the extent of intermolecular interactions. The value for PEN was found to be extremely high which indicates rigidity of the chain as well as sensitivity of the material to temperature changes.

Table 2 Activation energy of flow of PEN as a function of shear stress

Shear stress (MPa)	Activation energy of flow ($kJ\,mol^{-1}$)
0.30	257
13.84	267
27.39	263
40.94	258
54.48	253
68.02	247
81.57	242
86.08	240

Optical microscopy

Transmission optical photomicrographs taken from A1 cuts of samples moulded at three different mould temperatures are shown in *Figure 3*. For mould temperatures up to the T_g of PEN, ($T_{mould} \leqslant 120$°C) we observe a thin transparent skin, a transparent core and a dark intermediate region next to the broad surfaces of the samples at location no. 0 and next to all four surfaces of the samples at locations no. 3 and no. 4. At the four corners of the samples the dark regions are absent. These dark regions form parallel to the surface plane of the samples and are thickest midway between the corners and their thickness decreases towards the corners. They disappear at the four corners leaving a transparent continuous passage from skin to core. They are the thickest at the entrance region (location no. 0) and at the end of the converging region (location no. 3), where the material is subject to elongational flow. As will be shown later, these layers correspond to the three distinct morphological layers observed earlier in injection moulded slowly crystallizing polymers such as PPS, PEEK and PAEK[11-13]. They correspond to a rapidly quenched amorphous skin, a crystalline shear region and an amorphous core.

Figure 4 shows the combined effect of injection speed and mould temperature on the A1 cuts taken at locations no. 0, no. 3 and no. 4. It can be seen that the injection speed plays a role in the formation of the shear crystallized layers—as the injection speed decreases the thickness of the shear crystallized layers increases. This

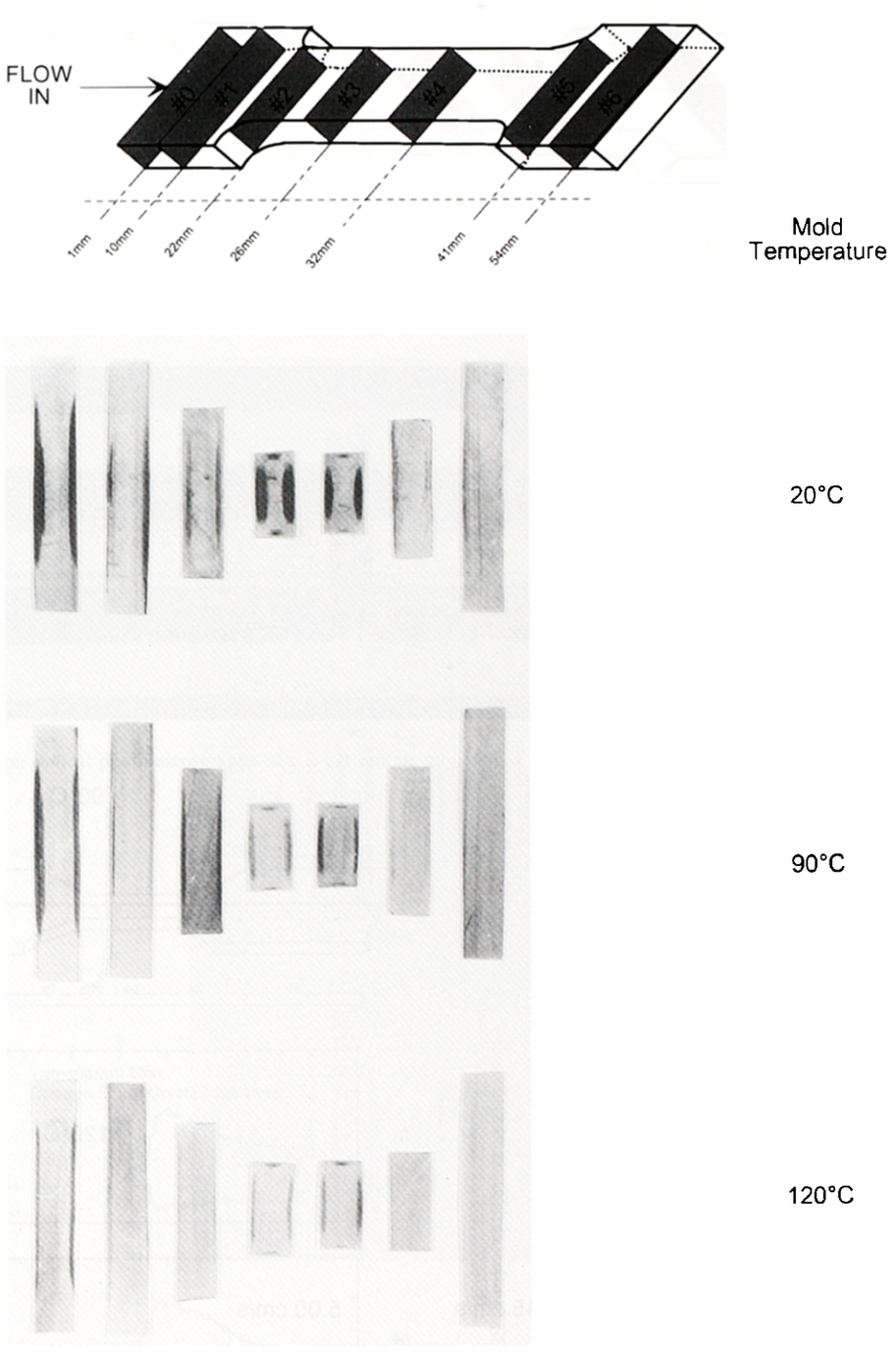

Figure 3 Transmission optical photomicrographs of the A1 cuts showing the effect of mould temperature on the formation of structure. Locations are as shown on the diagram

is particularly evident at low mould temperatures and at location no. 3 where sudden contraction of the cavity causes local acceleration of flow which enhances the elongational component of the flow field. This, in turn, significantly affects the structure formation. This effect, however, diminishes at 90 and 120°C. This relative insensitivity to the injection speed may be attributed partly to the decrease in the shear history with increasing mould temperature (as a result of reduction in average cooling rate and viscosity). In other polymers of similar crystallization characteristics (PPS, PEEK and PAEK) that exhibit much higher viscosities the influence of injection speed on the development of the shear crystallized layer and its thickness was much more pronounced even at high mould temperatures. The effect of increasing mould temperature manifests as a decrease in thickness of the skin layer and a shift in the location of the thickness maximum towards location no. 4.

The variation of this three-layer structure along the flow direction can be observed in *Figure 5*, where the transmission photomicrograph of the B cut of a sample moulded using the low injection speed at 20°C is shown.

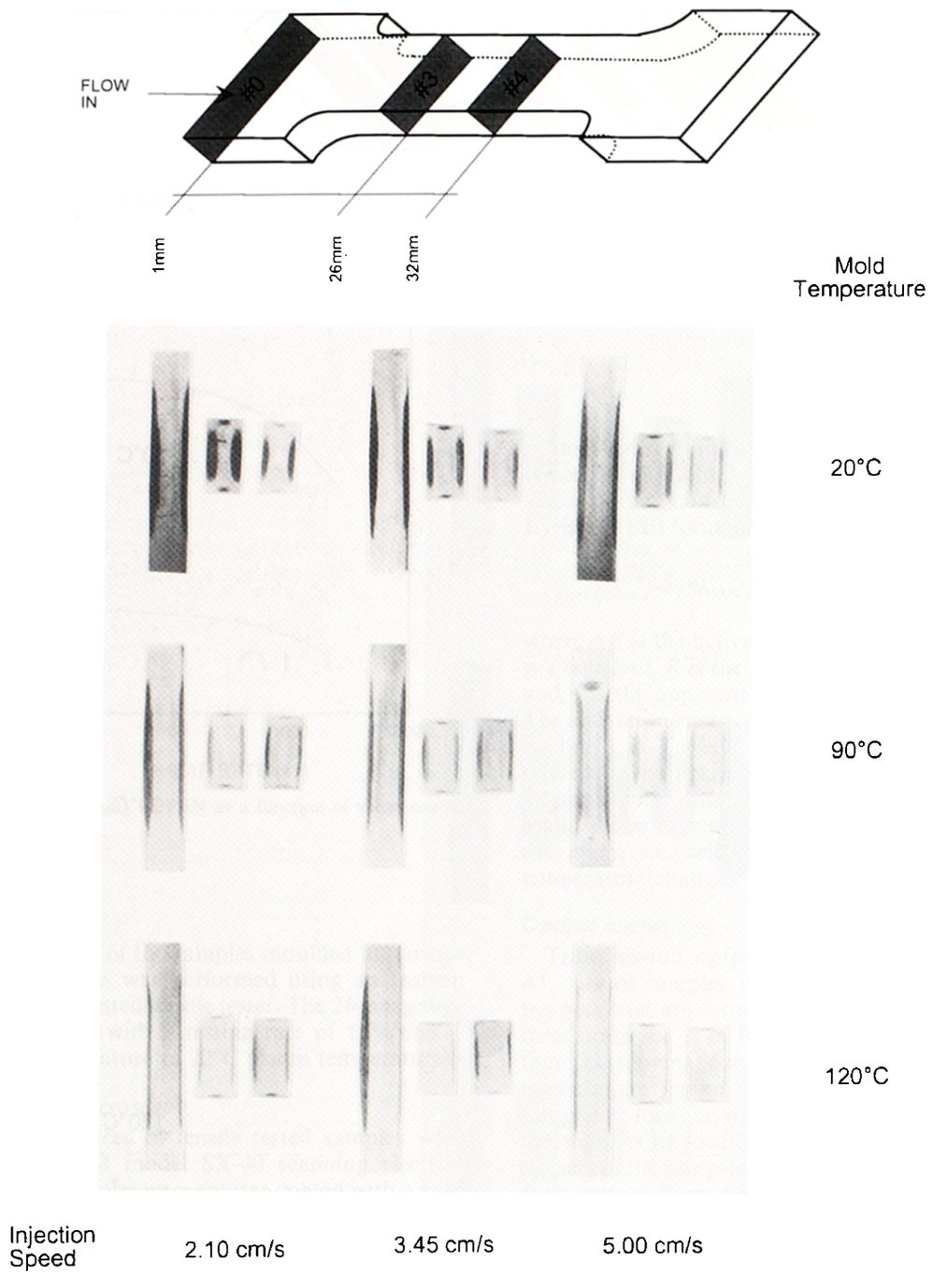

Figure 4 Transmission optical photomicrographs of the A1 cuts showing the combined effect of mould temperature and injection speed on the structure formation. Locations are as shown on the diagram

Stress crystallized layers just beneath the surface layers are present at the gate location and their thickness decreases along the flow direction and finally disappears well before the neck region. They reappear again at the neck region where elongational stresses are experienced by the flowing melt as a result of decreased cross-sectional area (which also increases overall cooling rates in the interior of the sample). *Figures 6–8* show the variation of the thickness of the crystalline and skin layers as a function of position and moulding conditions for B-cut samples. We can observe that both injection speed and temperature influence the crystalline layer formation. As the mould temperature decreases, both the crystalline layer and skin layer thickness increases. Similarly when the injection speed is lowered, the stress crystallized layers become more pronounced and are present throughout the flow direction. As indicated earlier, the formation of the crystallized layers appears to be a result of the stress history the polymer chains experience as they make their way through the narrow passages (runners, gates, etc.). In this particular mould design, the gate region is rather narrow which imparts significant shear and extensional

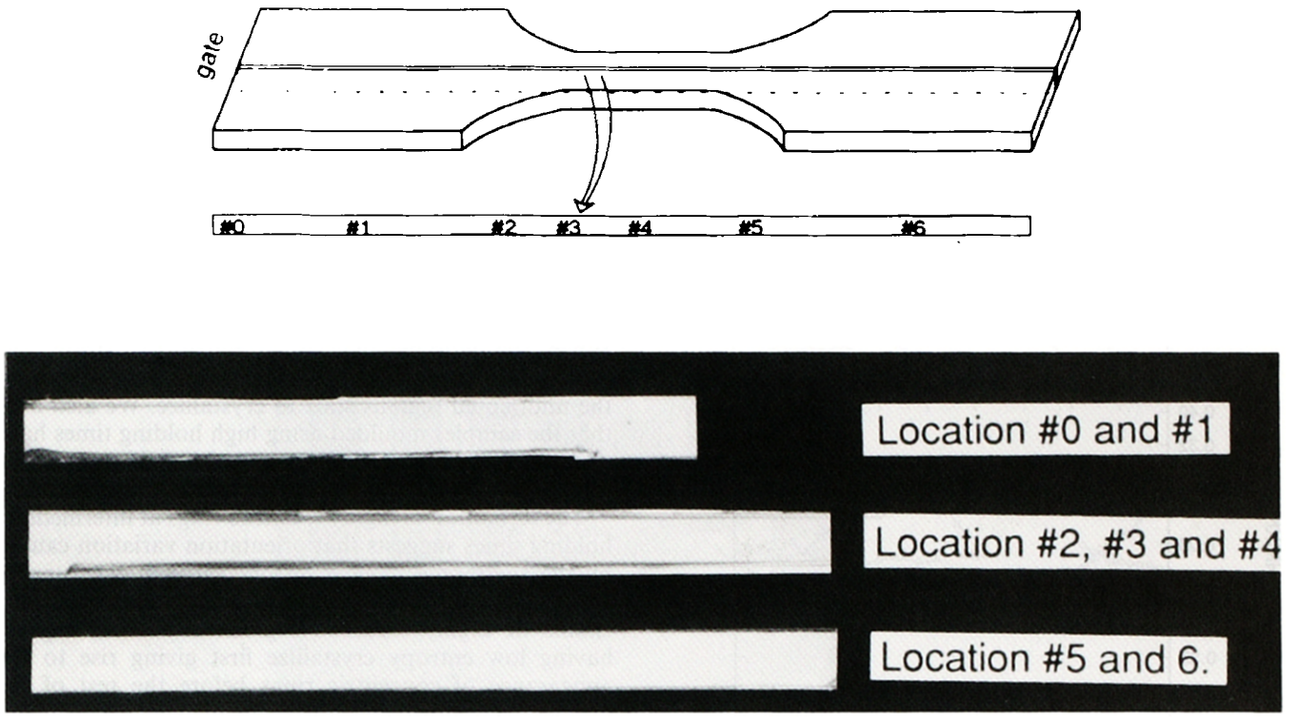

Figure 5 Transmission optical photomicrographs of a B-cut sample moulded at 20°C using the low injection moulding speed

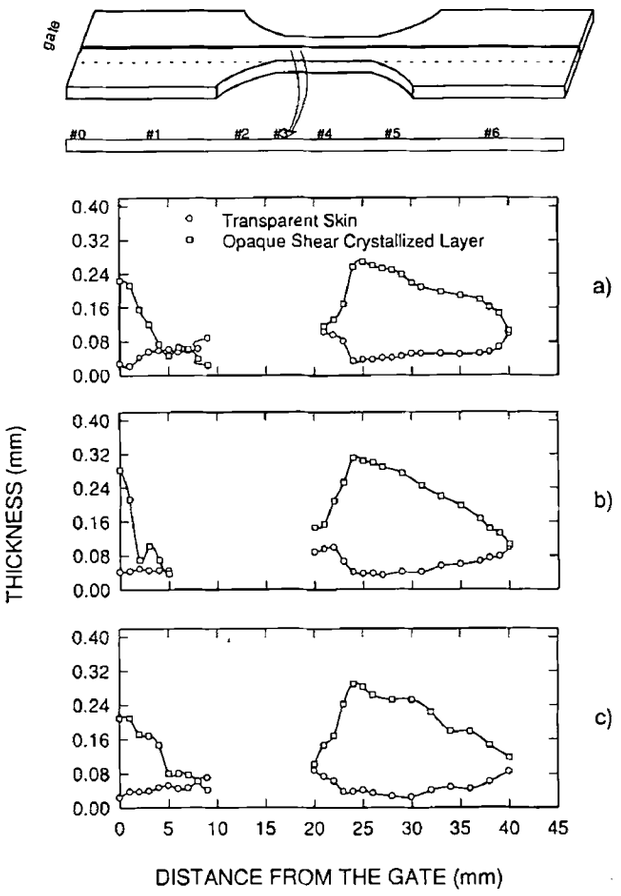

Figure 6 Thickness of the crystalline and skin layers measured form the B-cut samples moulded at 20°C using three different injection speeds: (a) low, 2.1 cm s^{-1}; (b) medium, 3.45 cm s^{-1}; (c) high, 5.00 cm s^{-1}

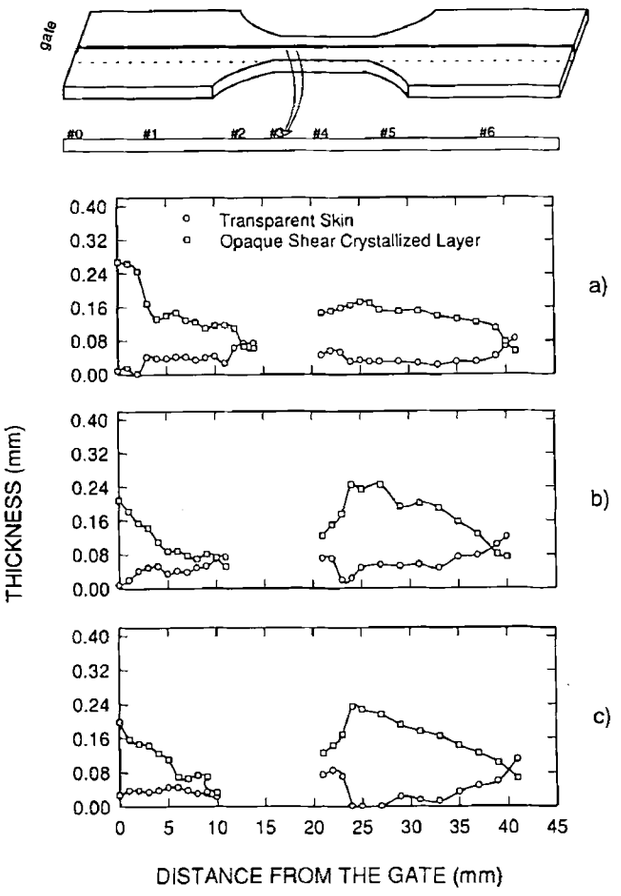

Figure 7 Thickness of the crystalline and skin layers measured form the B-cut samples moulded at 90°C using three different injection speeds: (a) low, 2.1 cm s^{-1}; (b) medium, 3.45 cm s^{-1}; (c) high, 5.00 cm s^{-1}

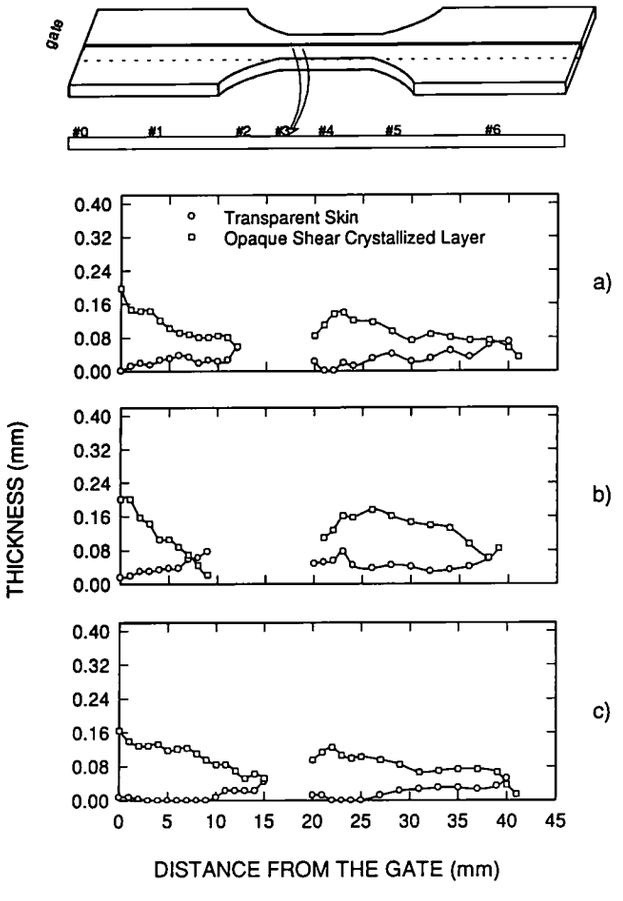

Figure 8 Thickness of the crystalline and skin layers measured form the B-cut samples moulded at 120°C using three different injection speeds: (a) low, 2.1 cm s^{-1}; (b) medium, 3.45 cm s^{-1}; (c) high, 5.00 cm s^{-1}

stress history to the polymeric chains before they enter the cavity. The appearance of the crystallized layers at locations downstream of the narrow passages is not surprising considering that they are formed by the orientation effects of the deformation field. We also note that there is a broadening of the crystalline region around the gate as the mould temperature increases. The sensitivity of the onset of crystallization to the mould geometry (hence stress history) can be seen at the region around the pressure transducer: there is a small but distinct difference, in the skin and crystalline layer thickness, between the flat side and transducer side of the mould (*Figure 5*). This is due to the small change in the flow channel thickness. Details of the mechanism will be discussed later.

Figure 9 shows the progression of crystallization with holding time in A1 cuts of samples moulded at 180°C. At this temperature we can still observe a basic three-layer structure in the samples having a 5 min holding time however, the thickness of the dark region is significantly reduced and it is very close to the skin of the sample. As the holding time is increased from 5 to 20 min the initially featureless core region gradually darkens. This darkening does not occur uniformly throughout the sample but occurs by forming thin darker layers making concentric elliptical rings in the interior. The darkest and the thickest of these layers is still located closest to the skin layer. Presumably, this layer formed during the injection step and the formation of thin interior layers may be explained at follows. Since the thermomechanical history plays an important role in the crystallization and the polymeric melt goes through the high stress regions in the gate and near the advancing frozen layer before reaching their final destination, they accumulate varying levels of orientation at different layers. But it appears that this thermomechanical history is not sufficient for them to crystallize during the injection step (with the exception of the layer closest to the surface) and when sufficient time is allowed at elevated temperatures these highly localized and oriented layers crystallize. When the holding time is extended to 20 min, the structure becomes uniformly crystalline and opaque as the unoriented regions start to crystallize. We also note that the samples moulded using high holding times have sink marks due to shrinkage of the material during thermally induced crystallization.

The formation of highly localized rings at intermediate holding times suggests that orientation variation caused by the thermomechanical history through the runners and gates reduces the conformational entropy of the chains at highly localized regions and these regions having low entropy crystallize first giving rise to the appearance of concentric rings before the rest of the sample crystallizes uniformly. As it can be seen from *Figure 10* the injection speed has no effect on the formation of the structure. This can be explained by the further decrease in the viscosity at this mould temperature, which causes a levelling of orientation. The absence of the injection speed effect also supports the fact that the rings are formed during the holding stage due to preferred thermal crystallization.

Figure 11 shows the progress of crystallization with holding time along the flow direction in the B cut samples moulded at 180°C. We observe the same structural progress: the sample exhibiting a basic three-layer structure at 5 min holding time converts to a multilayer structure (which indeed results from the sectioning of the ring structure along the centreline) at 10 min holding time before attaining a uniformly opaque appearance at higher holding times (20 and 30 min).

Thermal analysis

The d.s.c. scans of the A1-cuts show the average change in the thermal behaviour along the flow direction. Although each slice contains a large structural gradient, this analysis was done to elucidate the average changes that take place along the flow direction. *Figure 12* show such d.s.c. scans of a sample moulded at 20°C using a low injection speed. Near the gate (location no. 0) the d.s.c. spectrum indicates a T_g around 120°C and two cold crystallization peaks: one at around 170°C and a larger one at around 200°C. This is followed by a major melting peak around 265°C and a minor higher melting peak around 300°C. At locations no. 1 and no. 2 where the structure was uniformly transparent the higher temperature melting peak disappears and the lower temperature cold crystallization peak is also suppressed. The double cold crystallization peaks and double melting peaks become significant again at locations no. 3 and no. 4 where we have already observed the reappearance of the crystallized sublayer in the optical photomicrographs (*Figure 3*). We also observe that at locations no. 0, no. 3

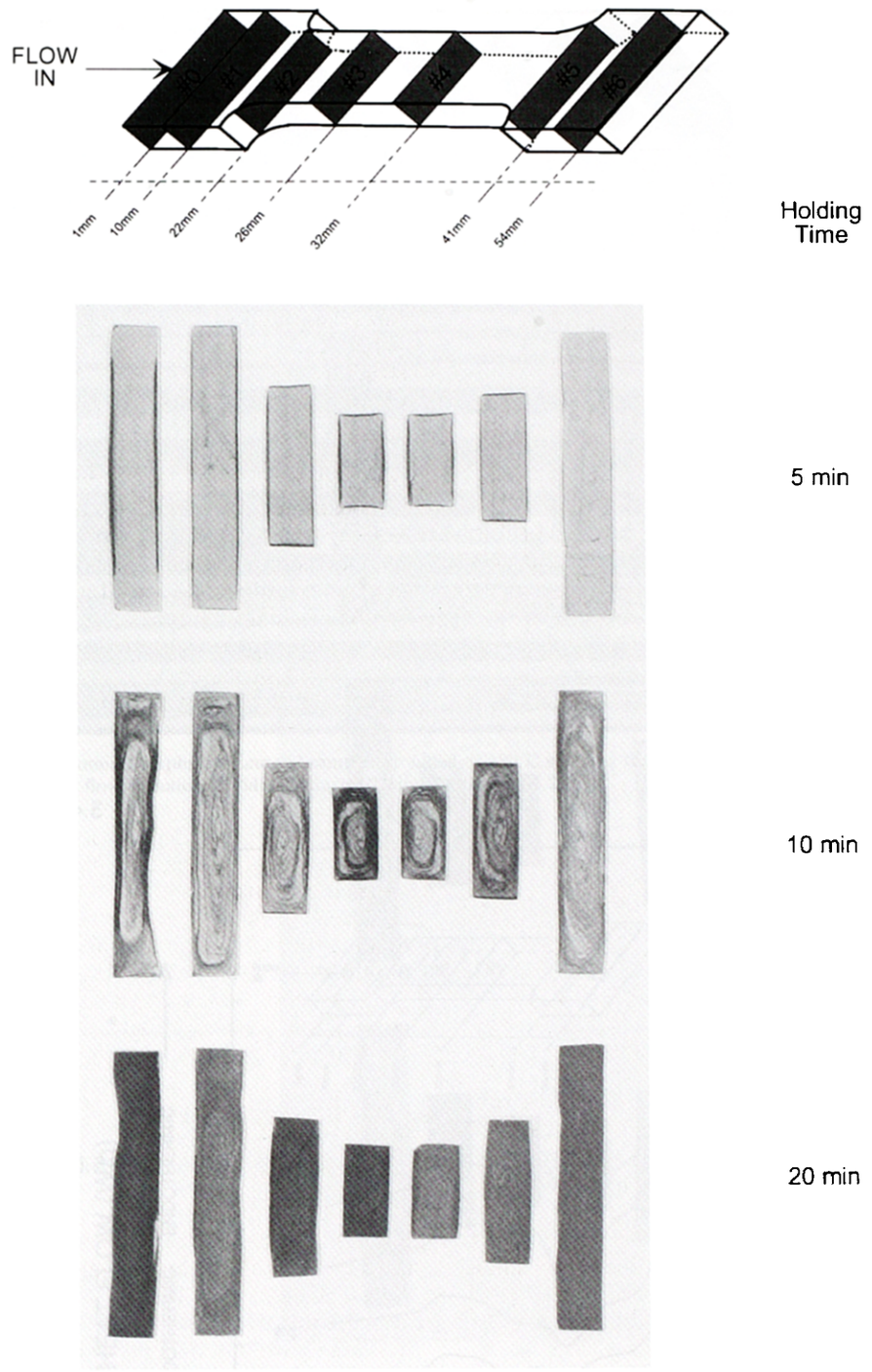

Figure 9 Evolution of structural gradients for the holding times shown in the transmission photomicrographs of the A1 cuts of a sample moulded at 180°C using the high injection speed

and no. 4 the area under the cold crystallization curve decreases which shows that the degree of crystallinity is higher at these locations. This behaviour suggests that the presence of the dark layer causes the formation of the lower cold crystallization peak and higher melting peak. To elucidate this further, we microtomed the location no. 3 of the same sample along the (FD-TD) plane into three slices: (1) skin; (2) core layers; and (3) stress induced crystalline dark layer, using Procedure A2. The d.s.c. scans of the core and shear regions are shown in *Figure 13* together with the d.s.c. scan of the A1 cut. The d.s.c. scans of the skin and core regions (the former was omitted for the sake of simplicity), which correspond to the transparent regions of the sample, were the same as amorphous PEN samples. However that of the shear region had a T_{cc} at 164°C and a distinct secondary melting peak at 301°C. These scans suggest that the overall d.s.c. curve is a consequence of the averaging of the different

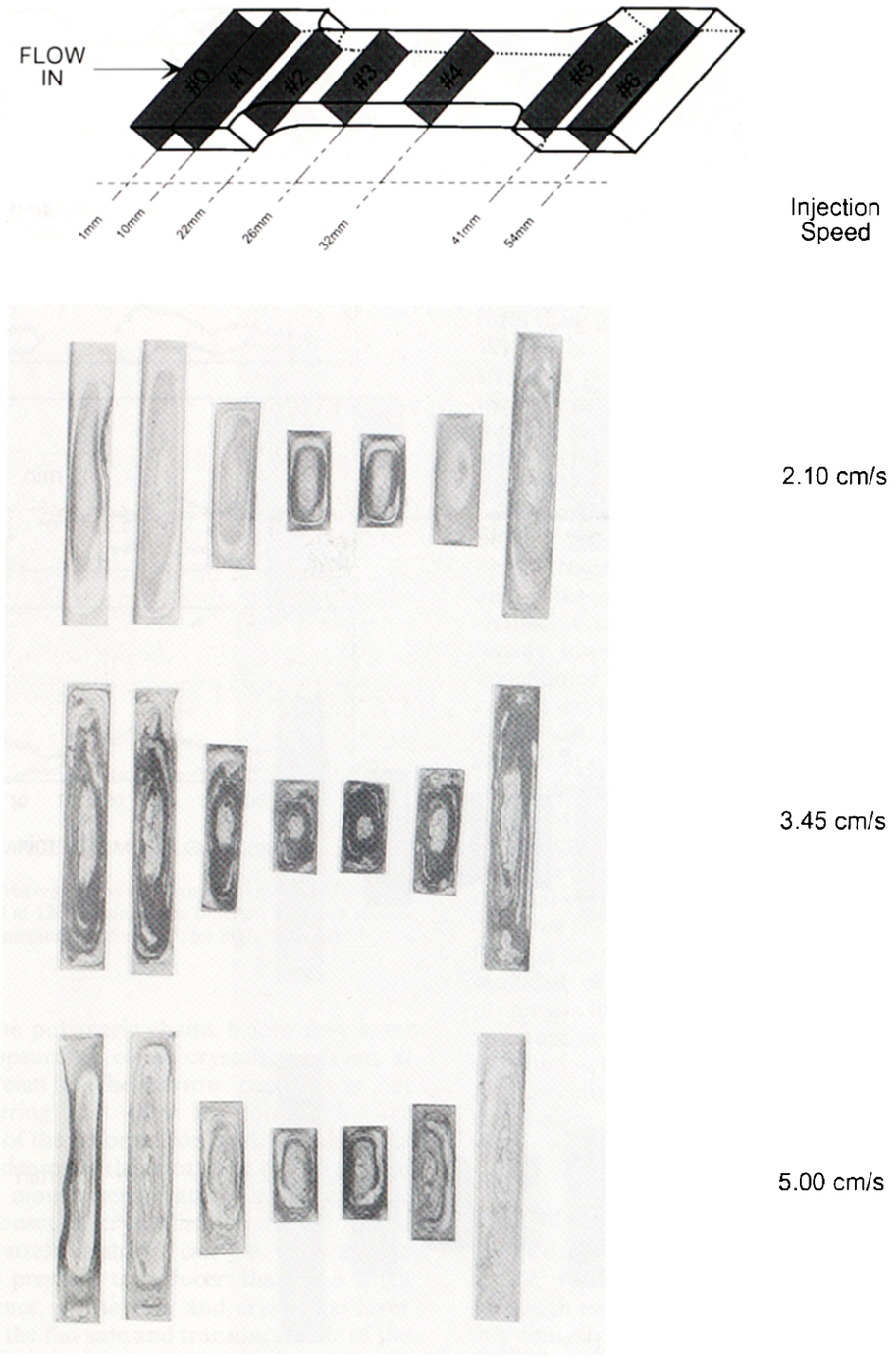

Figure 10 Transmission photomicrographs of A1 cuts showing the effect of injection speed on the structure development. Samples moulded at 180°C with a 10 min holding time

thermal characteristics of the two regions. The T_{cc} was unusually low and comparable to the temperatures observed during the solid state extrusion of PEN[8]. The lowering of T_{cc} during solid state extrusion was attributed to the stress induced orientation effects which justifies the formation of opaque crystalline layers at the locations where the stress history is maximum. Although a 20°C increase in the T_m with annealing[5] and secondary melting peaks having lower T_m were reported[7], a secondary melting peak having a higher T_m was never observed. This suggests the existence of a new crystal form or a population of more perfect crystals having thicker lamellae. The d.s.c. scans of the A1 cuts of samples moulded at 90 and 120°C had the same characteristics however, as will be shown later, their degree of crystallinity was lower.

The d.s.c. scans of the A1 cuts of samples moulded at 180°C using two different holding times are shown in

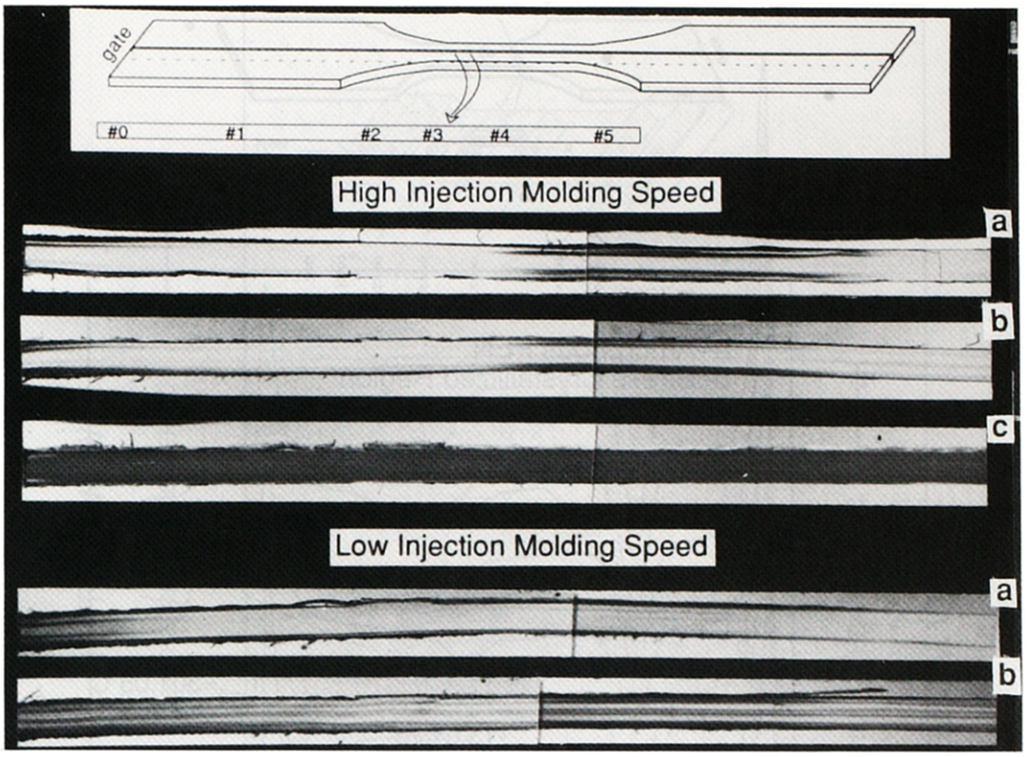

Figure 11 Transmission photomicrographs of B cuts of samples moulded at 180°C showing the effect of injection speed and holding time on the structures developed along the flow direction. Holding time: (a) 5 min; (b) 10 min; (c) 20 min

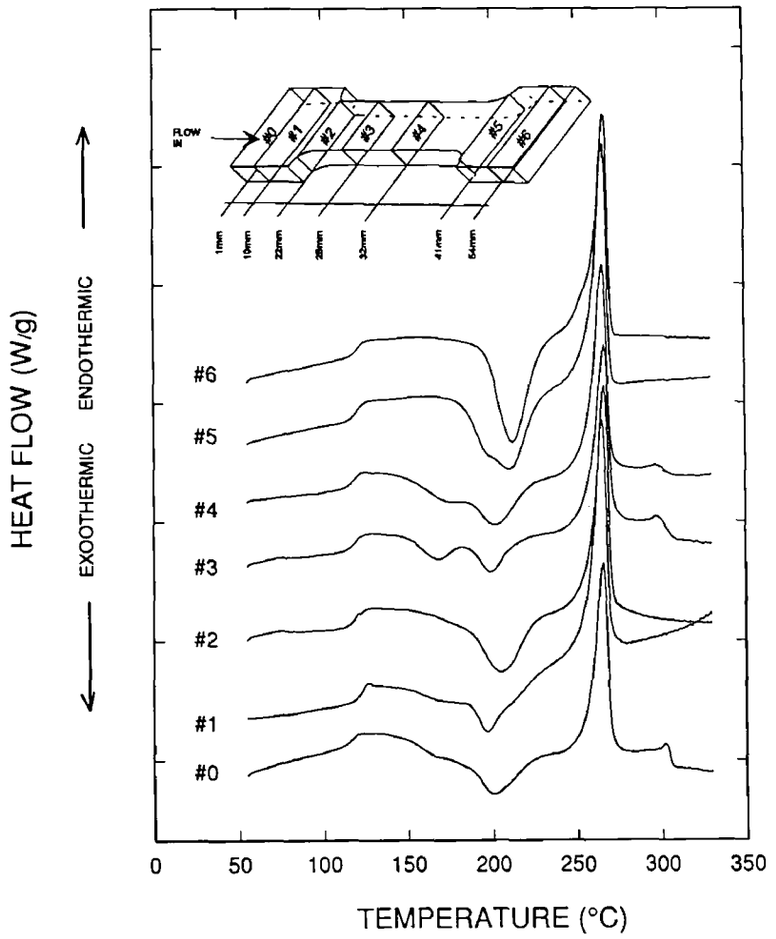

Figure 12 D.s.c. scans of A1 cuts taken from different locations of a sample moulded at 20°C using the low injection moulding speed

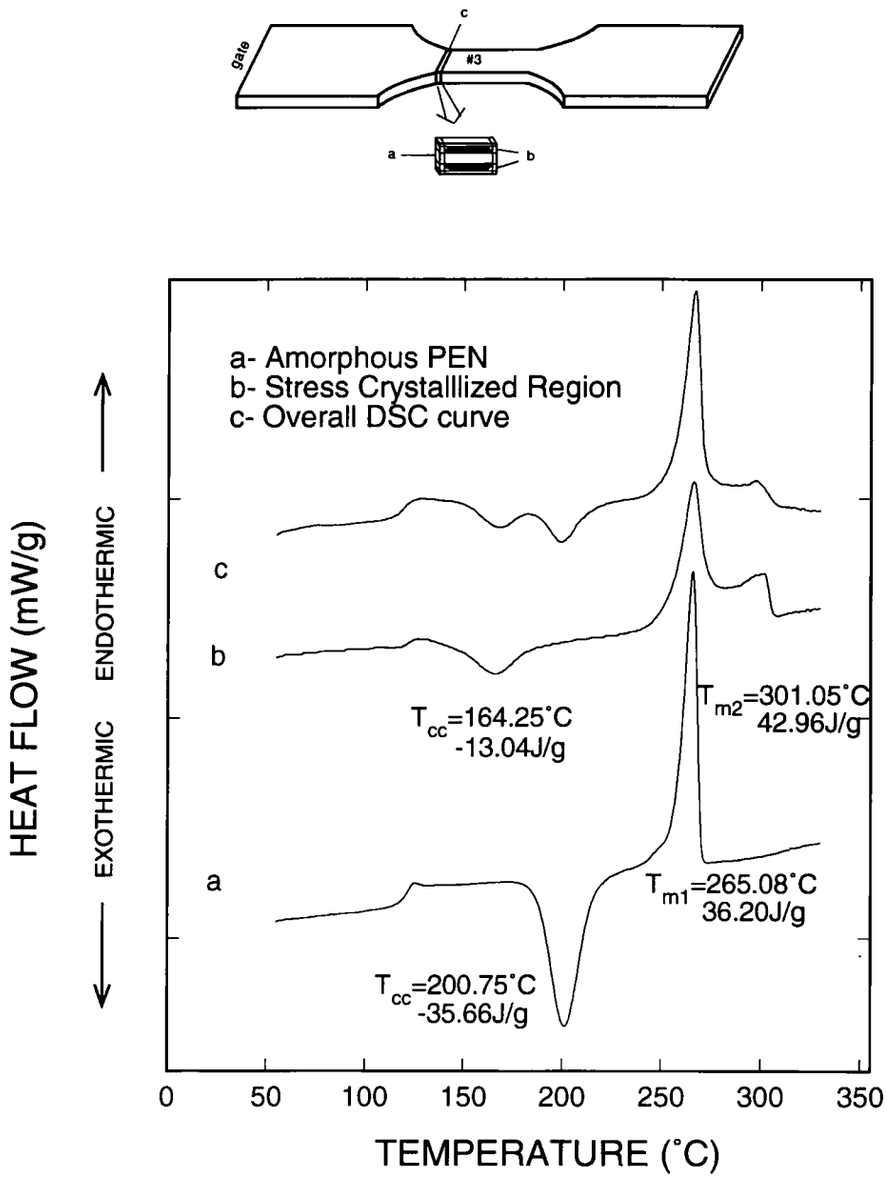

Figure 13 D.s.c. scans (a) of the A1 cut taken from location no. 3 of a sample moulded at 20°C using the low injection moulding speed, (b) of the crystalline region cut from the same sample using Procedure A2 and (c) of the amorphous skin and core regions cut from the same sample using Procedure A2

Figures 14 and *15*. The d.s.c. scans of the samples having a 5 min holding time are basically the same as those of amorphous PEN and do not depend on the location as was the case at low mould temperatures. Those of samples having a 30 min holding time are typical of PEN annealed at the same temperature and show a premelting peak around 179°C which is typical of annealed polyesters.

To compare the nature of the crystalline layers formed at mould temperatures around and below T_{cc} we followed the melting sequence of samples microtomed from location no. 3 of parts moulded at 20 and 180°C using Procedure B. *Figure 16a* shows a series of polarized transmission photomicrographs of a B-cut sample taken at different temperatures while it was being heated in the hot stage at a constant heating rate of 10°C min^{-1}. *Figure 16b* shows the temperature dependence of the depolarized light intensities at selected regions, namely skin, shear crystallized regions and core. These locations are indicated in *Figure 16a*.

In *Figure 16a* we can observe four different morphological layers identified as skin, shear, transition and core, with the last two being further divided into two sublayers. We did not observe any significant change in the morphology up to around 140°C (T_g). Above this temperature we observed a rearrangement at the core region which manifests as the partial melting of the second core sublayer. This is followed by the partial melting of the second transition layer at 190°C which leads to the onset of cold crystallization at 210°C (T_{cc}). At 260°C melting of the first crystal population (core) begins. With the melting of the first transition layer at 275°C the melting of the first crystal population is completed. At this temperature the skin layer starts to melt and the birefringence of the stress crystallized layer

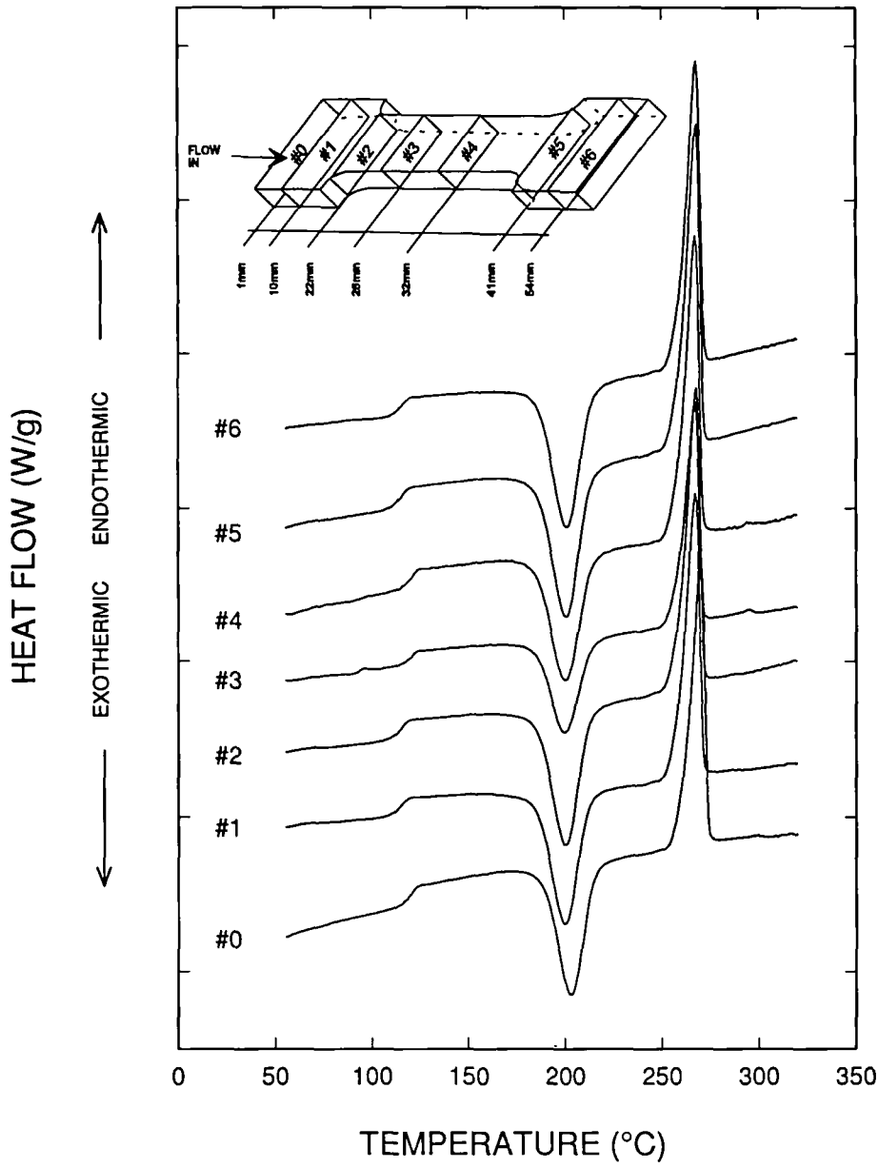

Figure 14 D.s.c. scans of A1 cuts taken from different locations of a sample moulded at 180°C using the high injection speed. Holding time = 5 min

begins to change. When the melting of the skin is finished the change in the birefringence is also completed. This justifies our earlier suggestion that the stress induced crystalline layer is a mixture of two populations melting at different temperatures. The low melting temperature fraction corresponds to those regions where the chains were originally oriented but remained amorphous until they were crystallized during the d.s.c. scan, whereas the high melting temperature fraction corresponds to the regions crystallized during the injection step into a different crystal lattice structure or into crystals having a different crystal size and orientation.

In *Figures 17a* and *b* a similar sequence is shown for a sample moulded at 180°C. We observe a similar crystallization behaviour. However the melting behaviour of this sample is quite different from the sample moulded at 20°C. Here the melting is along the whole thickness and crystal layers seem to follow the flow lines. The fact that the crystal layers begin to melt in between the flow lines might indicate that these regions are formed in an oriented state thereby having locally a slightly higher melting point. At this high mould temperature, we still observe the skin layer having a higher melting point but the highest melting point crystal fraction is not present. These differences in the melting behaviour can be explained by the differences in the thermomechanical histories of the two samples which represent the two extreme cases. The sample moulded at 20°C experiences the highest stress history as a result of fast cooling and this causes the formation of the shear crystallized layer near the skin. The sample moulded at 180°C experiences a relatively lower stress history as a result of a reduction in the average cooling rate. Under these conditions the structure of the part forms primarily as a result of thermally induced crystallization. However, there still is evidence of stress crystallization in the 'layered' melting

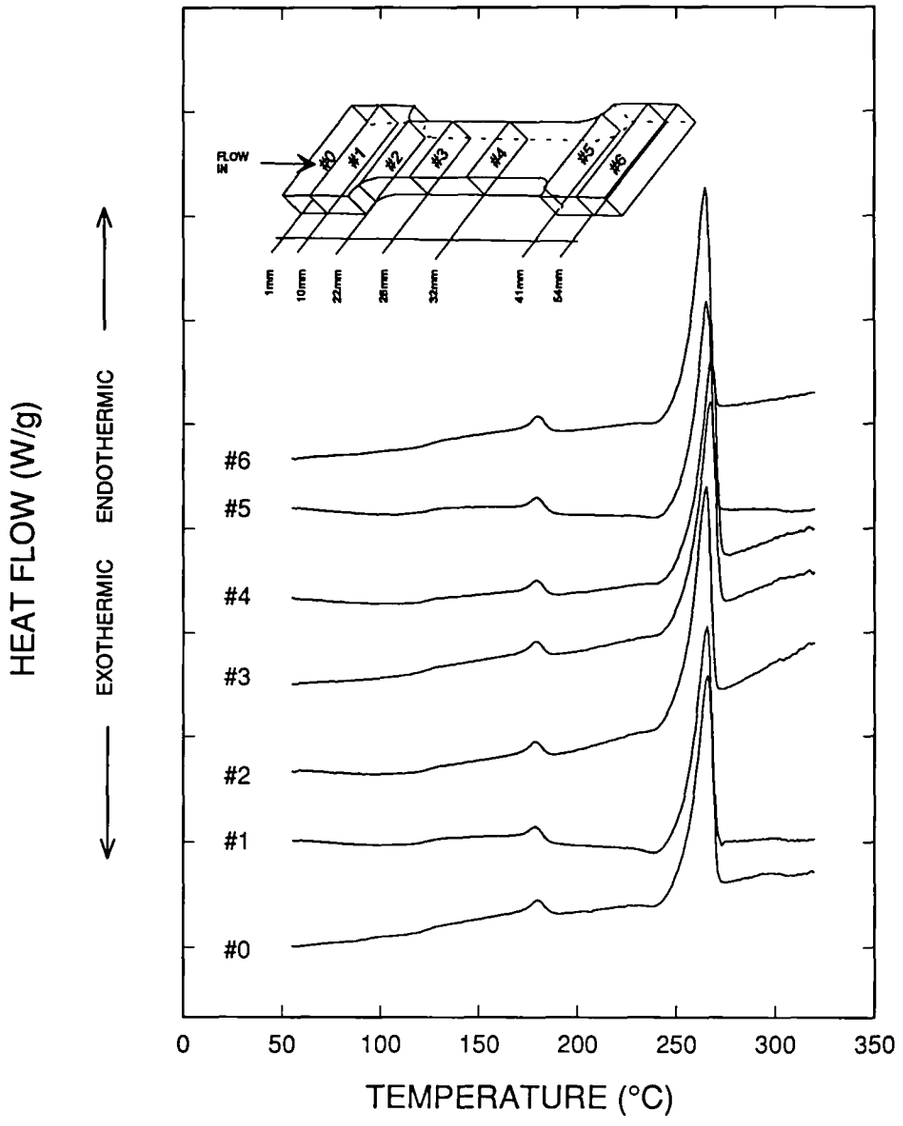

Figure 15 D.s.c. scans of A1 cuts taken from different locations of a sample moulded at 180°C using the high injection speed. Holding time = 30 min

sequence we observed. The regions that melt at higher temperatures probably have been nucleated by the orientation effects of the shear history.

The variation of the average degree of crystallinity along the flow direction, calculated from d.s.c. scans of the A1 cuts, is shown in *Figures 18* and *19*. At mould temperatures below the T_{cc}, it can be seen that crystallinity is highest at the gate (location no. 0) and at the end of the converging section (location no. 3) and generally it increases with decreasing injection speed. At 180°C the crystallinity profile along the flow direction is rather flat and the degree of crystallinity increases with increasing holding time.

Structural interpretation

We can explain the formation of the alternating amorphous crystalline amorphous morphology using TTT continuous cooling diagrams[18] which show the locus of points at which crystallization begins on a plot of temperature *versus* logarithm of time. When we superpose this curve with the cooling curve of the material within the mould, we can see if the crystallization (phase transition) is feasible: only if the two curves intersect does the material crystallize. The TTT curves are affected by the stress level. Increasing stress will lower the induction time and increase the crystallization temperature, i.e. it will shift the curves to the left and up. This approach was used by one of the present authors to interpret the crystallization in injection moulding of slowly crystallizing polymers[11-13]. *Figure 20* shows such diagrams for different regions of the sample. In *Figure 20a* we see the situation for the skin, the cooling rate and the stresses are the highest, however since the cooling rate is higher than the induction time the material does not crystallize. In the intermediate regions cooling rates become moderate however the stress level is still high and the material

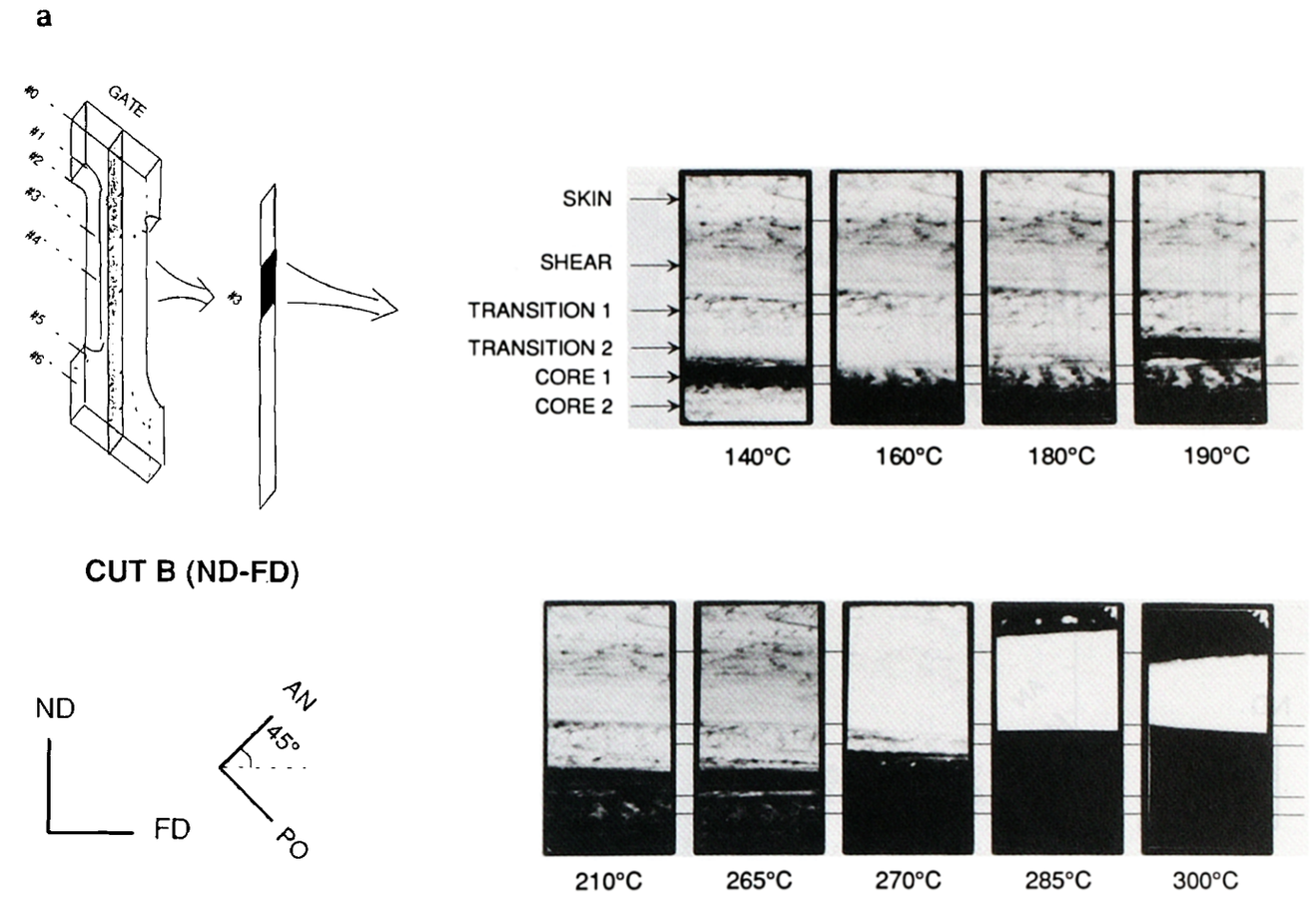

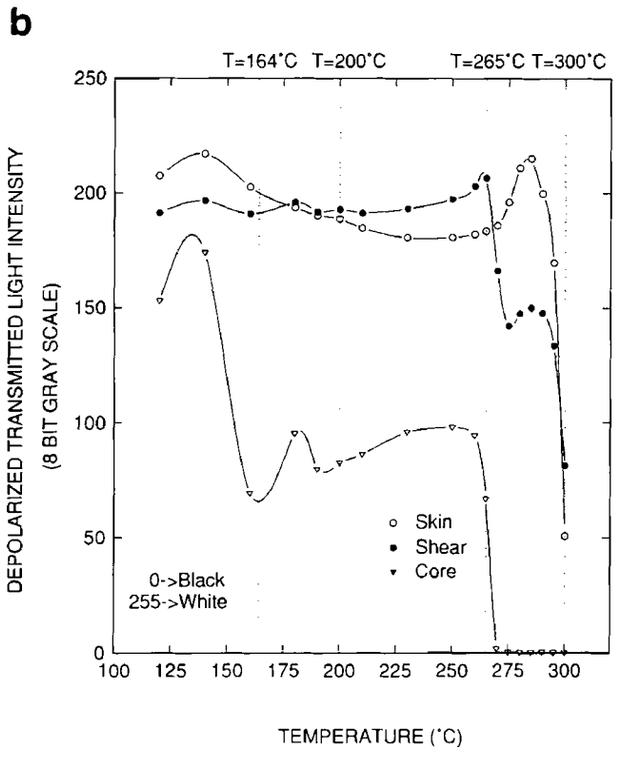

Figure 16 Transmission photomicrographs showing the melting sequence of a sample taken from location no. 3 using the B-cutting procedure (a). Evolution of depolarized transmitted light intensity with temperature (b). Sample moulded at 20°C using the low injection moulding speed

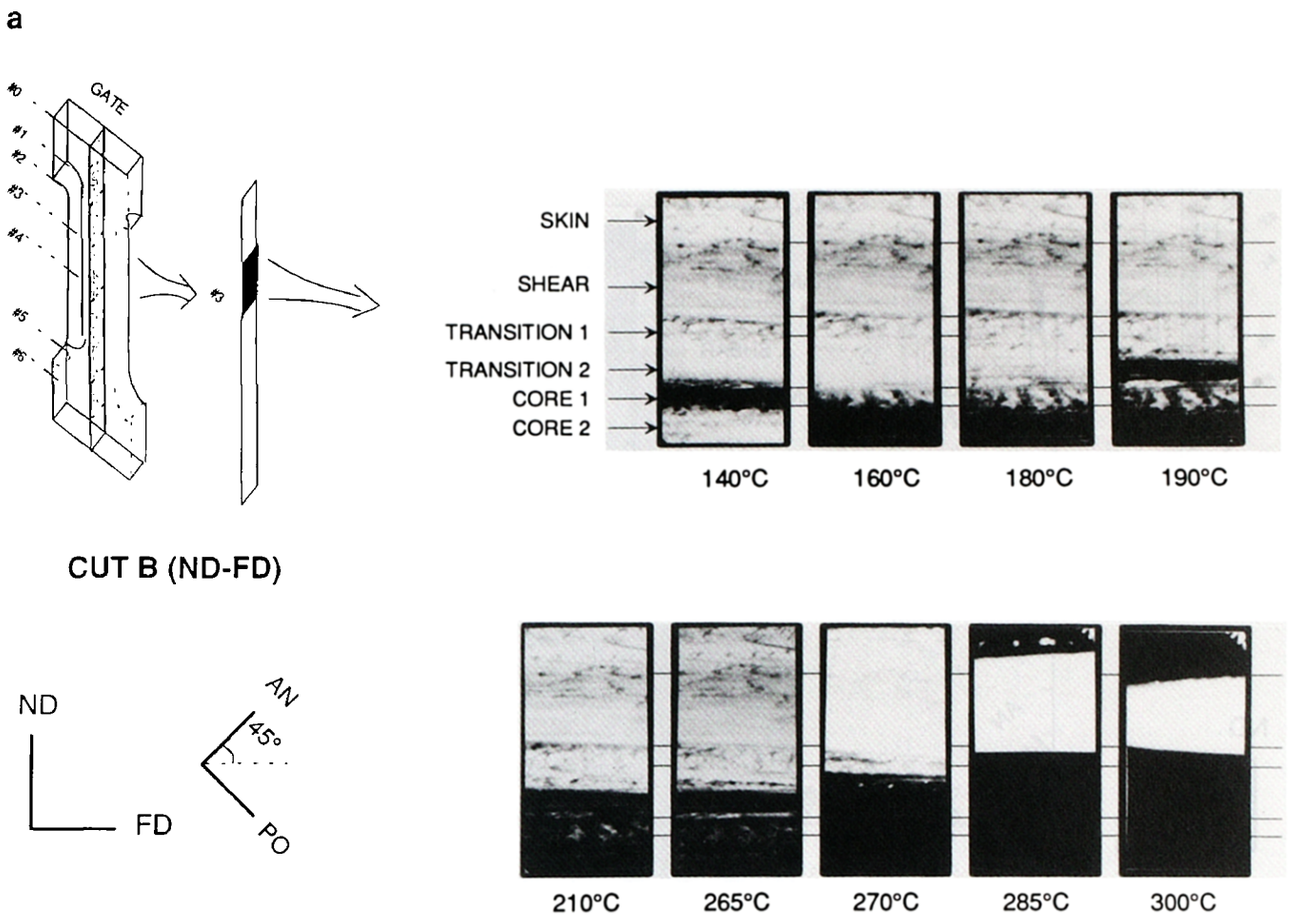

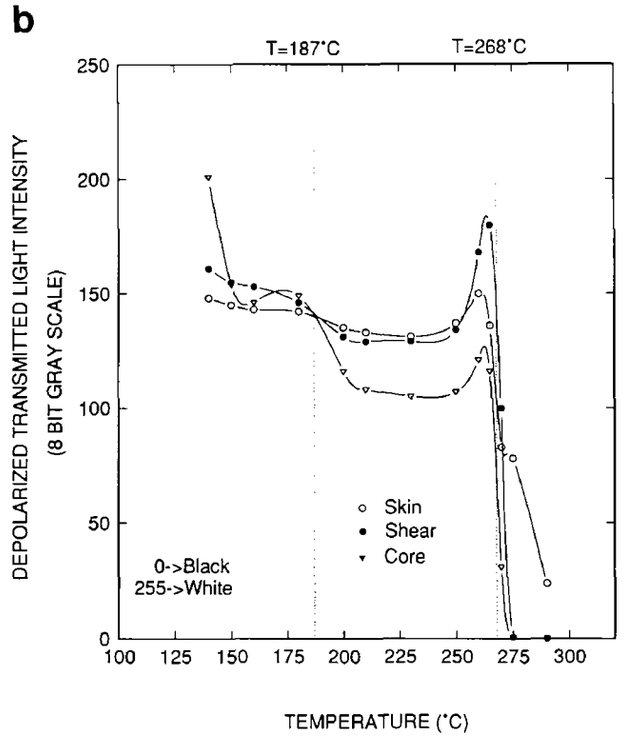

Figure 17 Transmission photomicrographs showing the melting sequence of a sample taken from location no. 3 using the B cutting procedure (a). Evolution of depolarized transmitted light intensity with temperature (b). Sample moulded at 180°C using the low injection moulding speed

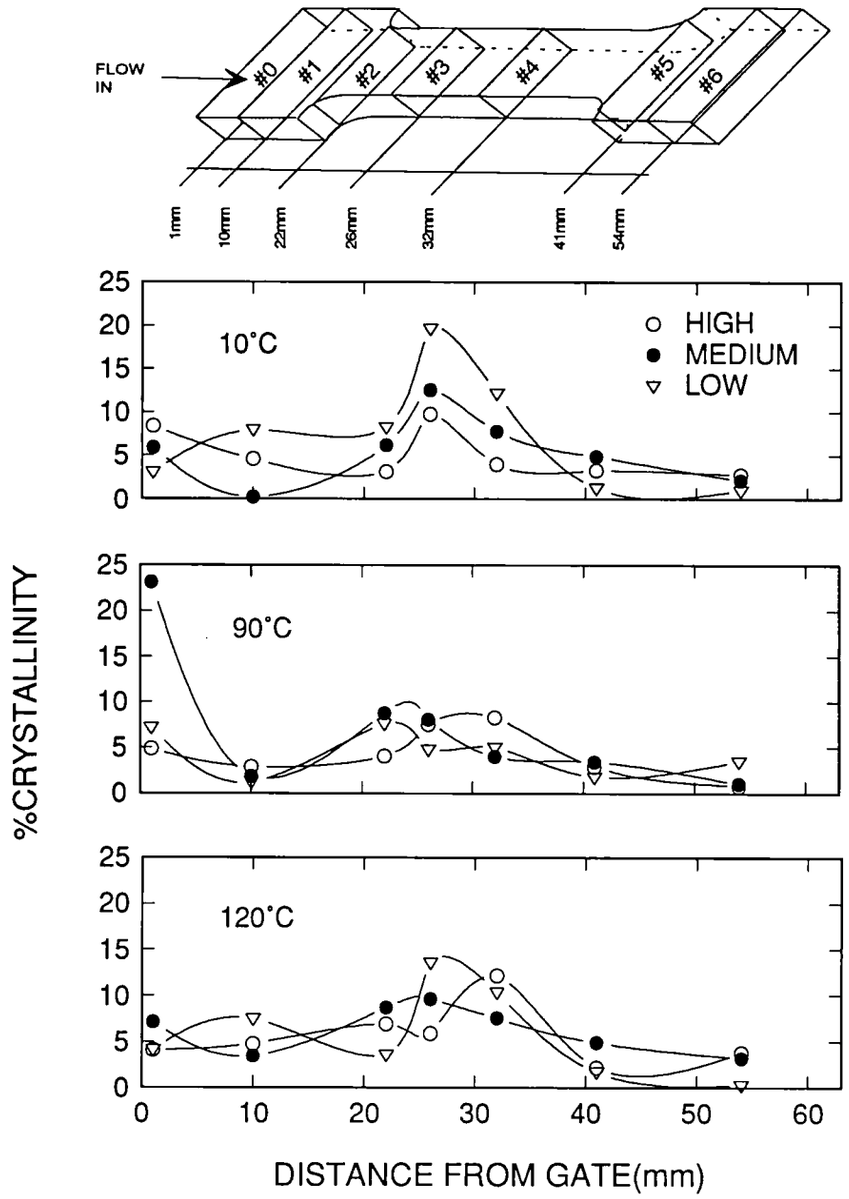

Figure 18 Effect of mould temperature and injection speed on the evolution of the average degree of crystallinity along the flow direction

crystallizes as shown in *Figure 20b*. Finally, cooling rate and stress levels are a minimum in the core due to low conductivity of the polymer and relaxation. This again prevents the material from crystallizing since the lowering of the cooling rate cannot compensate for the lowering of the crystallization temperature and increase of the induction time (*Figure 20c*). However, when the mould temperature is high enough for thermal crystallization to take place, the layers possessing sufficient stress history (but not sufficient crystallization time) crystallize first and this is subsequently followed by the crystallization of the relaxed layers.

Tensile testing

Typical stress strain curves of samples moulded at different mould temperatures are shown in *Figure 21*. We note that PEN behaves as a ductile material with a yield point below the T_{cc} and becomes brittle at 180°C. The tensile properties of the injection moulded samples are shown in *Figures 22* and *23*. For temperatures below T_{cc} there is no significant effect of injection speed and mould temperature on the tensile properties. However, at 180°C there is a significant decrease in the elongation at break due to the brittleness of the sample primarily caused by the presence of unoriented crystallites which formed as a result of thermal effects alone. *Figure 23* shows that the modulus and tensile strength of the sample increase while the elongation at break does not change significantly with increasing holding time at 180°C during which the material crystallizes.

Figures 24 and *25* show SEM photomicrographs of the fracture surfaces of the samples moulded using two

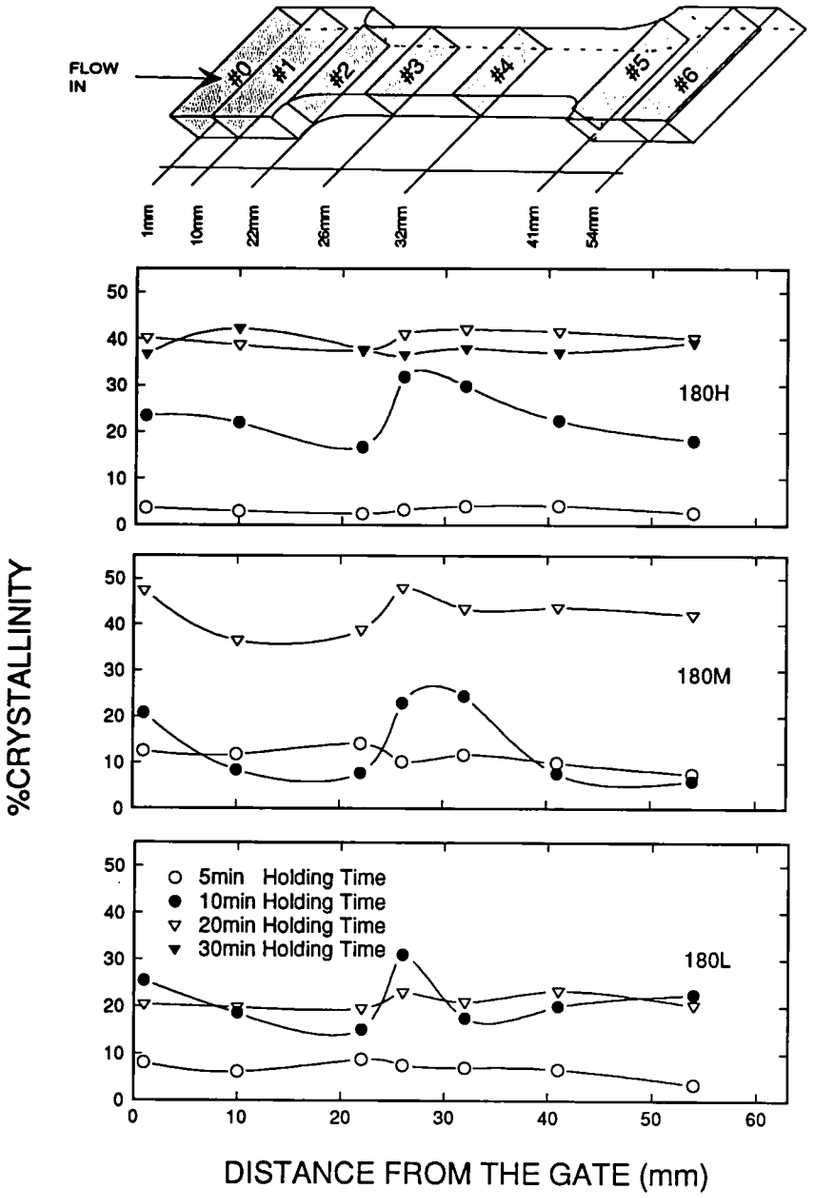

Figure 19 Effect of holding time and injection speed on the average degree of crystallinity along the flow direction for samples moulded at 180°C

different mould temperatures and high injection speed. *Figure 24* is typical of the samples moulded at mould temperatures below the onset of T_{cc} (20, 90 and 120°C). It should be noted that the shear crystallized regions appear delaminated near both sides of the polymer surface. Close examination of this fracture surface near the delaminated regions reveals highly layered internal structure resembling fracture surfaces of similarly processed thermotropic liquid crystalline polymers (*Figures 24a–d* are in order of increasing magnification). The amorphous skin and interior regions exhibit rather smooth surfaces and crystalline layers tend to split from the amorphous regions. This was also observed during the cutting procedures and we have to embed the samples in an epoxy matrix to prevent peeling. In all cases the failure was initiated by the cleavage at the sharp interface

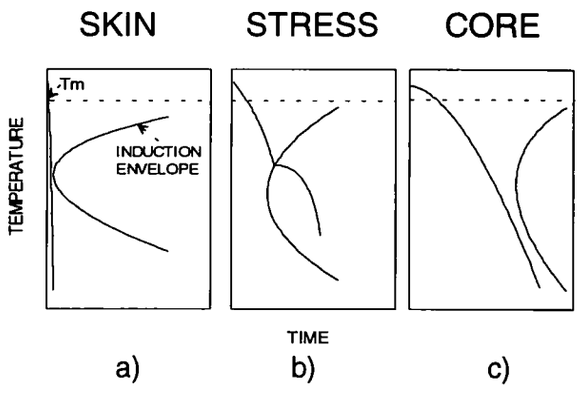

Figure 20 TTT curves corresponding to (a) skin, (b) shear and (c) core region of an injection moulded slowly crystallizing polymer

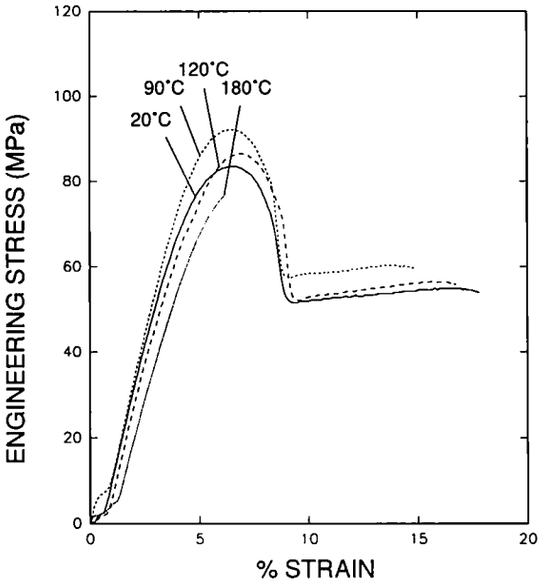

Figure 21 Typical stress–strain curves of samples moulded at different mould temperatures using the low injection speed. The holding time for the sample moulded at 180°C is 5 min

between the highly oriented crystals at the stress crystallized region and amorphous core. This can be explained by considering the material to be a composite structure: the skin and core consist of amorphous PEN which has a low modulus and high extensibility, whilst the shear region consists of highly oriented crystals having a relatively high modulus and low extensibility. This is also supported by the fact that the amorphous core is further stretched after the delamination. As will be reported in a subsequent paper[19], WAXS studies indicate that the naphthalene planes become parallel to the surface as a result of shearing and this causes delamination since there is minimal interchain forces between the chains oriented parallel to one another with naphthalene planes facing each other (graphitic or mica-like structure) and the broad surface of the sample. A highly stratified fracture surface also confirms this behaviour. At 180°C, which is around the onset of T_{cc}, we observe a brittle and uniform fracture (*Figure 25*).

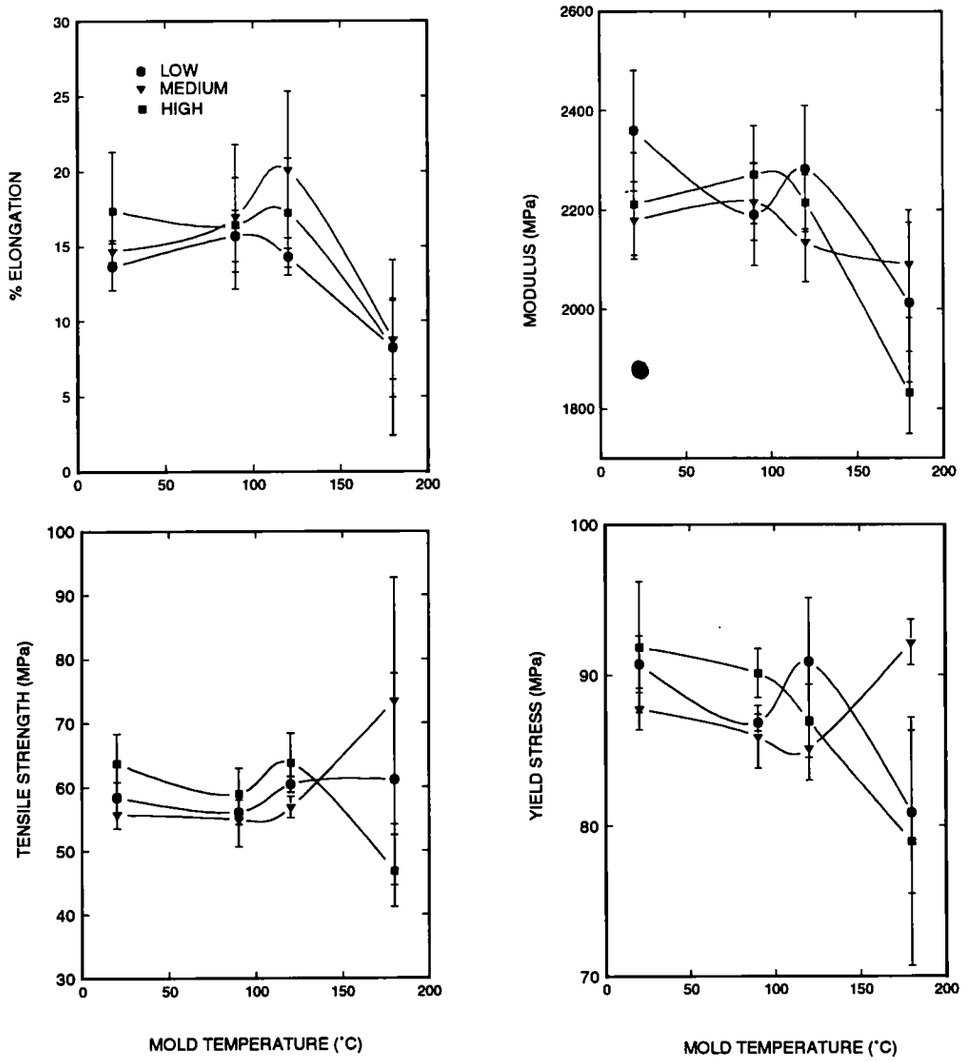

Figure 22 Combined effect of injection speed and mould temperature on the tensile properties of the samples. The holding time for the sample moulded at 180°C is 5 min

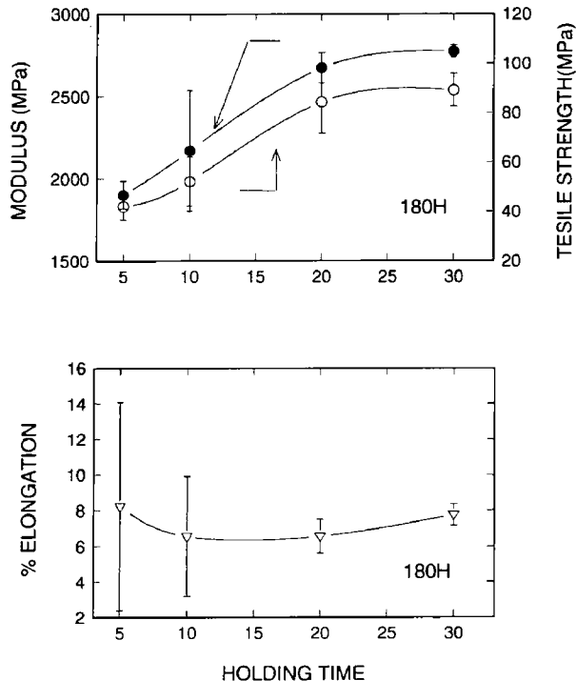

Figure 23 Effect of holding time on the tensile properties of samples moulded at 180°C

CONCLUSIONS

Injection moulded PEN exhibits distinct morphologies depending primarily on the mould temperatures used to produce them. Below T_{cc} the morphological layers of PEN follow the same amorphous–shear crystallized–amorphous sequence reported earlier. The d.s.c. and optical microscopy data suggest the formation of a

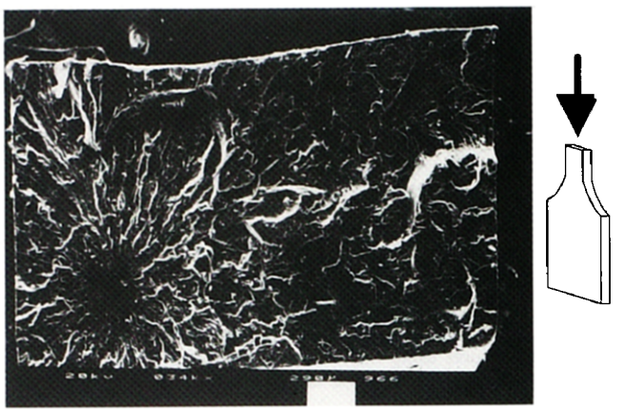

Figure 25 SEM photomicrograph of the fracture surface of samples after tensile testing. Sample moulded at 180°C using the high injection speed. Holding time = 20 min

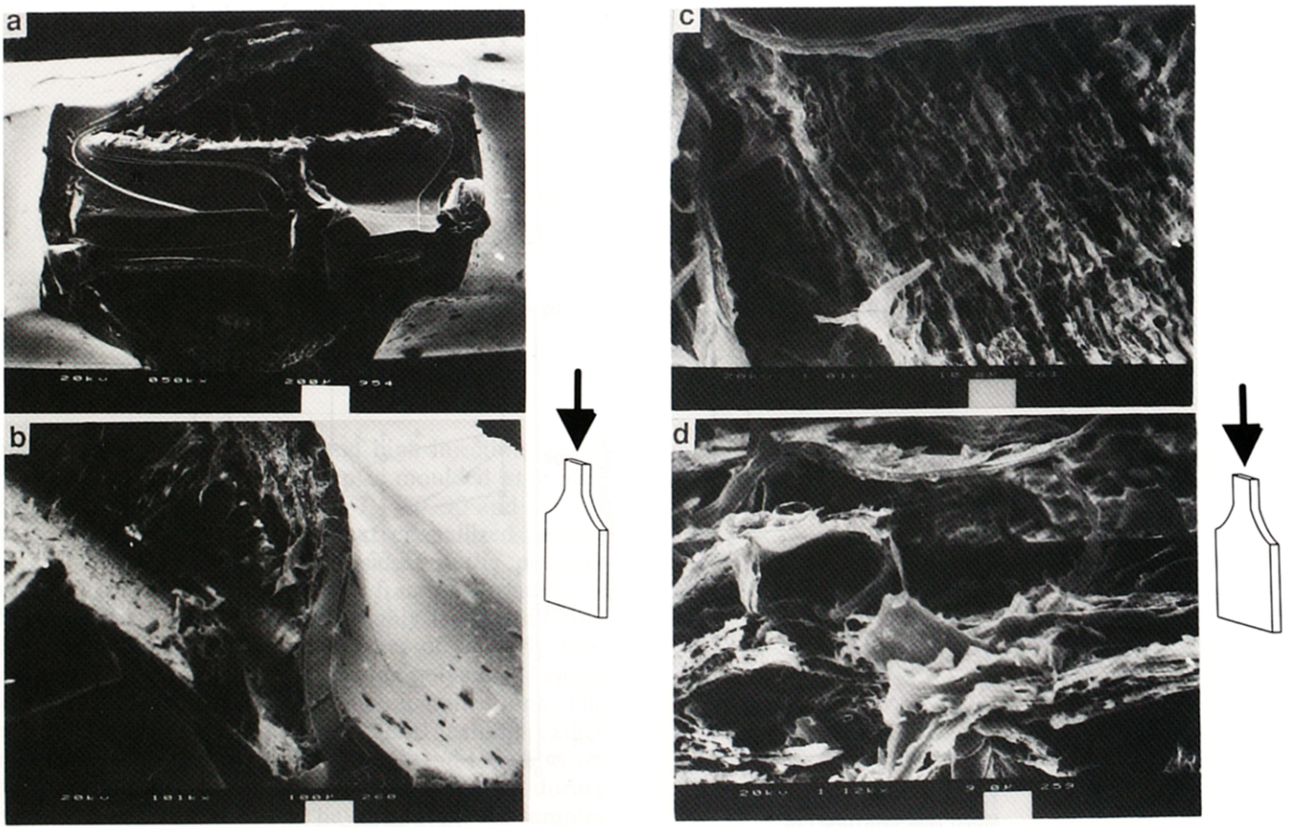

Figure 24 SEM photomicrographs of the fracture surface of samples after tensile testing. Sample moulded at 90°C using the high injection speed. (a)–(d) Increasing magnification

different crystal population upon injection moulding at mould temperatures below the T_{cc}. The crystalline layers having this form concentrate on the regions experiencing a high stress history during the filling stage. Around T_{cc} we observe a layered morphology dictated by a combination of thermal crystallization and orientation effects. The tensile properties and fracture mode of the injection moulded PEN follow the same transitions as the morphological features and change from ductile to brittle with increasing mould temperature. At mould temperatures below T_{cc} the crystalline layers peel away from the amorphous regions suggesting a high degree of orientation of these regions which causes naphthalene planes to align parallel to the cleavage surface. Within the processing window studied, we could eliminate the formation of this crystalline layer only by changing the mould geometry to that of a large ASTM dumb-bell having a thickness of 3 mm. This limits the use of PEN for the injection moulding of parts having narrow passages or thin sections due to the formation of a highly oriented crystalline layer which in turn affects the mechanical and optical properties of the parts.

ACKNOWLEDGEMENT

Funding for this research was partly provided by NSF Presidential Young Investigator Grant No. DDM-8858303.

REFERENCES

1 Cook, J. G., Hugill, H. P. W. and Low, A. R. *Br. Pat. 604073*, 1948
2 Ouchi, I., Aoki, H., Shinotsuma, S., Asai, T. and Hosoi, M. 'Proceedings of the 17th Japan Congress on Materials Research', 1974, p. 217
3 Buchner, S., Wiswe, D. and Zachmann, H. G. *Polymer* 1989, **30**, 480
4 Mencik, Z. *Chem. Prum.* 1967, **17**(42), 78
5 Zachmann, H. G., Wiswe, D., Gehrke, R. and Riekel, C. *Makromol. Chem.* 1985, Supple. 12, 175
6 Cheng, S. Z. D. and Wunderlich, B. *Macromolecules* 1988, **21**, 789
7 Cheng, S. Z. D., Janimak, J. J., Zhang, A., Guan, J. and Chu, A.-L. *Polym. Bull.* 1988, **20**, 449
8 Ghanem, A. M. and Porter, R. S. *J. Polym. Sci. B* 1989, **27**, 2587
9 Çakmak, M., Wang, Y. D. and Simhambhatla, M. *Polym. Eng. Sci.* 1990, **30**(12), 721
10 Çakmak, M., White, J. L. and Spruiell, J. E. *J. Polym. Eng.* 1986, **6**(4), 291
11 Hsiung, C. M., Çakmak, M. and White, J. L. *Int. Polym. Proc.* 1990, **5**(2), 109
12 Hsiung, C. M., Çakmak, M. and White, J. L. *Polym. Eng. Sci.* 1990, **30**(16), 967
13 Hsiung, C. M. and Çakmak, M. *J. Appl. Polym. Sci.* 1993, **47**, 125, 149
14 Rosato, D. V. and Rosato, D. V. 'Injection Molding Handbook', Van Nostrand, 1986
15 Katti, S. S. and Schultz, J. M. *Polym. Eng. Sci.* 1982, **22**(16), 1001
16 Hsiung, C. M. and Çakmak, M. *Polym. Eng. Sci.* 1991, **31**(19), 1372
17 Vinogradov, V. M. and Malkin, A. Y. 'Rheology of Polymers', MIR, Moscow, 1980
18 Spruiell, J. E. and White, J. L. *Polym. Eng. Sci.* 1975, **15**, 660
19 Ulcer, Y. and Çakmak, M. *Polymer* to be submitted